Catal Lett (2009) 127:437–443
DOI 10.1007/s10562-008-9734-8

Anchoring $RhCl(CO)(PPh_3)_2$ to $-PrPPh_2$ Modified MCM-41 as Effective Catalyst for 1-Octene Hydroformylation

Wei Zhou · Dehua He

Received: 6 August 2008 / Accepted: 14 October 2008 / Published online: 1 November 2008

Abstract $RhCl(CO)(PPh_3)_2$ was anchored to diphenylphosphinopropyl-modified ($-PrPPh_2$) mesoporous silicate MCM-41. Infrared spectroscopy was applied to monitor the multi-step assemble of the complex by assigning critical absorptions. The prepared catalyst was employed in 1-octene hydroformylation and showed high conversion of substrate as well as high selectivity of nonyl aldeydes (>97%) along with several stable catalyst cycles. Rhodium leaching in the reaction liquids was determined by mass spectroscopy, which was found extremely low. The catalyst showed higher activity and lower metal loss than the analogue by nano SiO_2 as support, probably as a result of the confining of molecular sieves with ordered pores.

Keywords Rh–P complex · Diphenylphosphinopropyl modification · MCM-41 · Hydroformylation · 1-Octene · Leaching

1 Introduction

Hydroformylation [1] of α-olefin allows producing higher aldehyde (or alcohol if further hydrogenation takes place) with one more carbon than the initial employed olefin. Hydroformylation products are widely employed as solvent, plasticizer, or the raw materials for the detergent fabrication. At present, the catalysts for the industrial hydroformylation are mainly rhodium complexes [2], for example the Wilkinson's catalyst $RhCl(PPh_3)_3$. Rhodium-catalyzed hydroformylation goes under mild reaction conditions and presents high alkene conversion as well as high selectivity of aldehydes. However, like many homogenous catalytic processes, the industrial hydroformyaltion suffers from the difficult catalyst separation. Therefore, heterogenization of the rhodium complex is a very meaningful work. Silica-based mesoporous molecular sieves are promising as support for immobilizing homogeneous catalysts [3], owing to their superiorities such as high surface area, thermal-/solvo- stabilities, and uniform pore size distribution. So far, various rhodium complexes have been anchored to mesoporous silicates. Peng et al. [4] anchored two Rh–P complexes to amino-functionalized MCM-41 and MCM-48 through Rh–N coordination. The catalysts were employed in 1-hexene hydrformylation within several runs but revealed obvious active species leaching. Huang et al. [5] reported the immobilization of rhodium to aminopropyl-modified MCM-41. The catalyst was respectively employed in the hydroformylation of 1-octene and styrene under optimized reaction conditions. However, the rhodium leaching degree was lack of evidence. In a recent work, Li and Kawi [6] reported the direct synthesis of SBA-15-supported Wilkinson's catalyst and its application in 1-stryene hydroformylation. Rhodium was also anchored to the hybridized SBA-15 by chelating of rhodium with amino-containing dendrimers. The rhodium leaching was minimized as a result of chelation. Marteel et al. [7] reported MCM-41-anchored Pt/Sn–P complex and its application in 1-hexene hydroformylation in supercritical carbon dioxide. There were no active species leaching data, and the specific catalyst activity was not comparable with rhodium-based catalysts. Sandee and co-workers [8] reported the Rh–P/N complex anchored to silica through

W. Zhou · D. He (✉)
Innovative Catalysis Program, Key Lab of Organoelectronics and Molecular Engineering of Ministry of Education, Department of Chemistry, Tsinghua University, Beijing 100084, China
e-mail: hedeh@mail.tsinghua.edu.cn

sol–gel technology. The sum rhodium leaching from catalysts recycles seems a little high (1% for each catalyst cycle).

Previous researches suffer from rhodium leaching during the catalyst cycles, leading to the catalyst activity decrease. One reason might be that rhodium was anchored to the support by Rh–N coordination. It is well acknowledged in the organometallic chemistry, phenyl phosphine ligands are very effective in forming stable transition metal complexes [9] owing to the conjunction of phosphorous *p* electrons with phenyl π electrons. So far, few researchers have devoted to the direct anchor of rhodium complex to phosphino-functionalized mesoporous silicate. In the present research, diphenylphosphine ligands (–PPh_2) will be connected with propyl-modified MCM-41 through an organometallic route. Coordination of a rhodium complex, $RhCl(CO)(PPh_3)_2$, is afterwards carried out to produce a MCM-41-anchored Rh–P complex catalyst throught Rh–P bonding. The catalyst will be used in the 1-octene hydroformylation, and metal leaching during the reaction will be a main concern. Nano SiO_2 will be also employed as support for comparison.

On the other hand, it has been a central difficulty in-situ characterizing the multi-step assemble of organometallic complex into the mesoporous silicates so as to clarify the structure formed inside the pores. In the present paper, infrared spectroscopy will be adopted to monitor the multi-step assemble of Rh–P complex to hybridized MCM-41 or SiO_2 by assigning critical absorptions. We would like to present the strength of IR spectroscopy in characterizing the surface properties of porous materials.

2 Experimental

2.1 Preparation of Catalysts

Preparation of MCM-41-anchored Rh–P complex catalyst is illustrated in Scheme 1. Parent MCM-41 was synthesized according to the literature methods [10, 11]. In a typical synthesis, ammonia (aq.) and cetyltrimethylammonium bromide (CTABr) were dissolved in distilled water under vigorous stir. Tetraethylorthosilicate (TEOS, Acrös) was then added dropwise. After continuous stir for 2 h, a gel with a molar composition of SiO_2:CTABr:NH_4OH:H_2O = 1:0.12:8:114 was obtained. The gel was then transferred into a Teflon-lined autoclave and was then heated at 383 K for 72 h. The solid product was recovered by filtration, washed with deionized water until the filtrate was neutral, and dried. The as-synthesized material was calcined at 823 K for 6 h in air with a temperature-programmed rate of 1 K min^{-1}. Organic functionalization of MCM-41 was finished by the grafting method [12]. One gram of MCM-41 was refluxed with 2 mL 3-chloropropyltrimethoxysilane (97%, Acrös) in 100 mL dehydrated toluene for 24 h. Diphenyl phosphine ligands connection was finished by mixing excessive $LiPPh_2$ [13] with chloropropylated MCM-41. The mixture was stirred at room

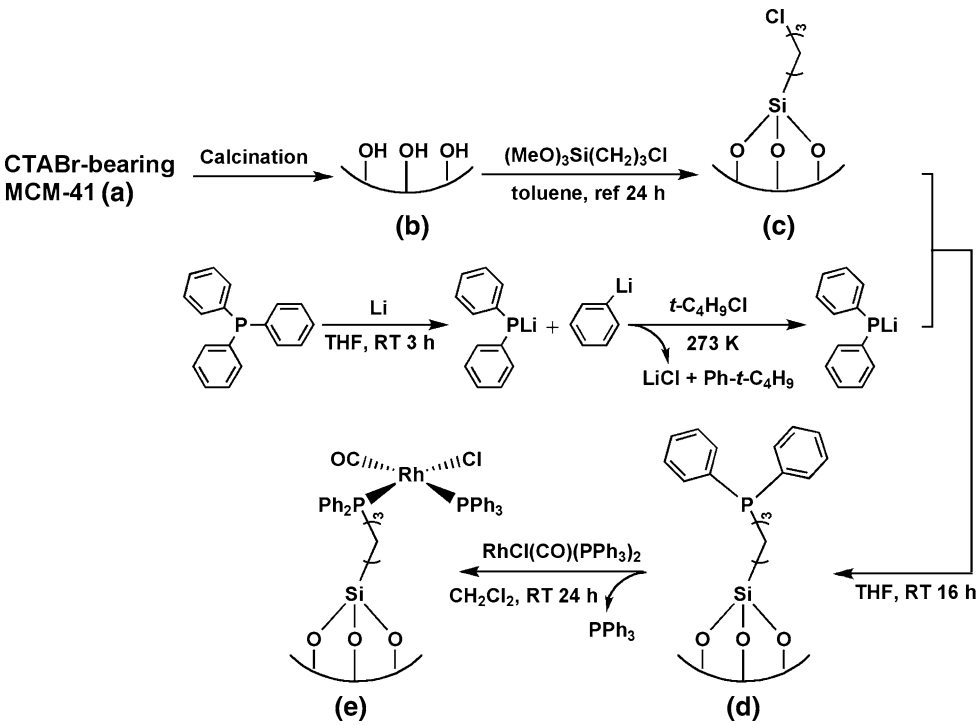

Scheme 1 Preparation of M–*Pr*PPh_2Rh catalyst

temperature for 16 h. Finally, the resulting solid was mixed with $RhCl(CO)(PPh_3)_2$ (Strem) in CH_2Cl_2 and stirred at room temperature for 24 h. As shown in Scheme 1, (c) and (d) were respectively washed in a Soxhlet's extractor for 12 h to remove physisorbed species. Final catalyst (e) was washed, assisted by an ultrasonic device, to remove uncoordinated ions [11]. The prepared MCM-41-anchored Rh–P complex catalyst is denoted as M–PrPPh$_2$Rh.

As comparison, nano SiO_2 (15 nm, $S_{BET} = 300\ m^2\ g^{-1}$, $D_{BJH} = 18.6$ nm, Tianjin Chemical Research and Design Institute) was also employed as support. The immobilization of $RhCl(CO)(PPh_3)_2$ to diphenylphosphinopropyl-modified SiO_2 was quite similar to the catalyst preparation described above. Nano SiO_2-anchored Rh–P complex catalyst is denoted as S–PrPPh$_2$Rh.

2.2 Characterization of Catalysts

Powder X-ray diffraction (XRD) data at low angles were collected on a Rigaku D/max-RB diffractometer at a scan solution of $2°\ min^{-1}$ with CuKα radiation ($\lambda = 0.1542$ nm). XRD characterization was powered at 40 kV and 100 mA. Fourier-transform infrared spectrometry (FT-IR) was operated on a Perkin SpectrumOne spectrometer by KBr wafers. Isothermal nitrogen sorption at 77 K was performed on a Micromeritics ASAP 2010 analysis system; the BET (Brunauer–Emmett–Teller) and the BJH (Barrett–Joyner–Halenda) methods were applied for the specific surface area and pore size distribution calculations, respectively. The immobilized Rh content was determined by the inductive coupling plasma-atomic emission spectroscopy (ICP-AES) method on an IRIS Intrepid II spectrometer (TJA Solutions). Rh leaching in the reaction liquids was determined by ICP mass spectroscopy (ICP-MS).

2.3 Hydroformylation of 1-Octene

1-Octene hydroformylation was carried out as follows. Five milliliters of 1-octene (Acrös, 99%) was mixed with 15 mL toluene (A.R.) in a 100 mL autoclave and catalyst was added. The autoclave was then sealed and syngas ($H_2/CO = 1$) was injected at lower than 278 K to replace the air inside the autoclave (3×). The autoclave was heated to 393 K and the syngas was injected to 5 MPa; the electromagnetic stir was started. At the end of the reaction, the autoclave was cooled to lower than 278 K and the pressure was released; 0.785 g isopropanol (A.R.) was added as internal standard. The resulting mixture was analyzed by a GC equipped with an SE-30 capillary column. In the catalyst recycle experiments, the separated catalyst was above all washed by toluene under ultrasonic washing.

3 Results and Discussion

3.1 Characterization Results

3.1.1 XRD Characterization

XRD patterns (Fig. 1) of both parent MCM-41 (a) and M–PrPPh$_2$Rh (b) revealed three well-resolved reflections with Miller Indexes (100), (110), and (200), characteristic of typical hexagonal structure. The d_{100} reflection is associated with the pore size of the material with the hexagonal symmetry by the equation [9]:

$$a_0 = \frac{2}{\sqrt{3}} d_{100} \quad (1)$$

where a_0 is the unit cell parameter. It equals to the pore size plus wall thickness. The d_{100} reflection appeared at $2\theta = 2.20°$ for the catalyst M–PrPPh$_2$Rh, which shifted a little to higher 2θ than corresponding reflection from the support. This indicates the decrease of pore size, according to Eq. 1. The grafted species onto the inner surface will decrease the pore size (Table 1 for D_{BJH} data), and they also lead to the shrinkage of the unit cell [12].

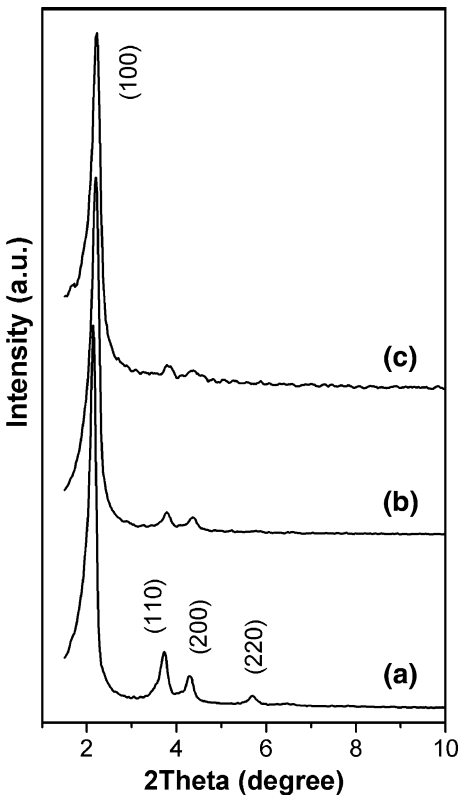

Fig. 1 XRD patterns of parent MCM-41 (**a**), M–PrPPh$_2$Rh catalyst (**b**), and M–PrPPh$_2$Rh catalyst after six runs in 1-octene hydroformylation (**c**)

Table 1 Textual properties of parent MCM-41 and M–*Pr*PPh_2Rh catalyst

	a_0[a] (nm)	S_{BET} ($m^2\ g^{-1}$)	D_{BJH} (nm)	V_P (cc g^{-1})	T_w (nm)	Rh (wt%)
MCM-41	5.40	755	2.75	0.52	2.65	–
M–*Pr*PPh_2Rh	4.64	693	2.52	0.43	2.14	1.5

[a] Calculated by Eq. 1. S_{BET} BET specific surface area; D_{BJH} BJH primary pore diameter; V_P single point total pore volume; T_W hexagonal phase wall thickness equalled to $a_0 - D_{BJH}$

3.1.2 FT-IR Spectroscopy

Figure 2 is the IR spectra [14] of parent and modified MCM-41, evidencing the multi-step assemble of Rh–P complex to diphenylphosphinopropyl-modified MCM-41. See Scheme 1 for correspondence of samples.

(a) *CTABr-bearing MCM-41*. Intensive ν_{as}(C–H) at 2,925 cm^{-1} and ν_s(C–H) at 2,854 cm^{-1} were shown. The rocking of long chain alkyl revealed three neighboring peaks at 1,491 cm^{-1}, 1,480 cm^{-1}, and 1,468 cm^{-1}. These IR absorptions were assigned to surfactant CTABr. ν(N–H) was overlapped by ν(O–H) at 3,433 cm^{-1} and was not clearly observed.

(b) *Calcined MCM-41*. The infrared absorptions of C–H stretching and rocking vibrations described in template-bearing MCM-41 (a) almost vanished, implying the successful removal of template.

(c) *Chloropropylated MCM-41*. After chloropropylation of MCM-41 by the grafting of siliane, ν_{as}(C–H) and ν_s(C–H) reappeared at 2,960 cm^{-1} and 2,852 cm^{-1}, respectively. The scissoring of propyl gave several peaks at ca. 1,444 cm^{-1}. ν(C–Si) was observed at 694 cm^{-1}, while ν(C–Cl) was found at 648 cm^{-1}. The above infrared absorptions were original from the 3-chloropropyltrimethoxysliane, which suggested the organic functionalization was successful. Noticeably, the peak intensity at ca. 966 cm^{-1}, characteristic of modifiable silanols [15] of MCM-41, was decreased after the silane grafting. This also implies the successful grating since the silanols reacted with silane.

(d) *M–PrPPh_2 (diphenylphosphinopropyl-modified MCM-41)*. After the connection of diphenyl phosphine ligands with chloropropylated MCM-41, the product revealed ν(C–P) at 745 cm^{-1} and δ(Ar C–H) at 865 cm^{-1} [16]. Two neighboring peaks, found at 3,075 cm^{-1} and 3,061 cm^{-1}, could be assigned to the over tone contributed by the aromatic stretching of C=C and C–H bonds from single-substituted benzene. The aromatic ν(C=C) resulted a broad infrared absorption at ca. 1,483 cm^{-1}, which might be finely composed of several peaks. The conjugation of *p* electrons from phosphorous and π electrons from phenyls had amplified this ν(Ar C=C) absorption. Owing to the electron-donating effect of the ligands, ν(C–Si) was increased after ligands connection (from (c) to (d)) [17].

(e) *M–PrPPh_2Rh (final catalyst)*. After rhodium complex immobilization (e), the ν(Ar C=C) absorption was somewhat weakened (from (d) to (e)). This might because the metal cation withdrew electrons and thus decreased the electron density of the phenyl rings [17]. ν(C=O) original from the rhodium complex was observed at 1,977 cm^{-1} (see insert). ν_{as}(C–H) shifted to lower wavenumber from 2,938 cm^{-1} to 2,928 cm^{-1}, indicating the electron-withdrawing effect contributed by the cation decreased the polarity of C–H bond. This means the complex has an interaction with the immobilized ligand so this electron induction could be performed, which implies the successful anchor of Rh–P complex.

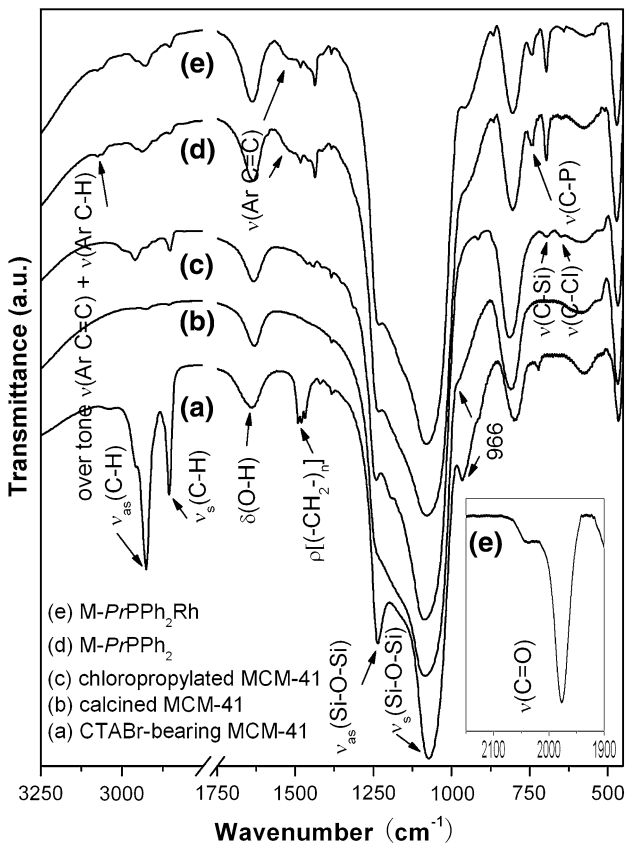

Fig. 2 IR spectra monitoring the multi-step assemble of Rh–P complex assemble. Inset: an enlarged area showing the stretching of carbonyl

In addition, the most intensive infrared absorption in the saturated region of 1,325–990 cm^{-1} showed the stretching of molecular sieve SiO_2 framework. The peak at 465 cm^{-1}

was assigned to the δ(Si–O–Si) [18]. Hereby the multi-assemble of Rh–P complex has been monitored by FT-IR spectroscopic characterization. The immobilization of $RhCl(CO)(PPh_3)_2$ to diphenylphosphinopropyl-modified nano SiO_2 could be similarly monitored by FT-IR, which showed very similar IR spectra (not shown).

3.1.3 N_2 Adsorption/Desorption Analysis

Figure 3 shows the isotherms of parent MCM-41 and the M–*Pr*PPh_2Rh catalyst. The insert is pore size distribution of the catalyst. The isotherms are both of type IV with a H1 hysteresis according to the IUPAC classification [19], typical of ordered mesoporous solids. This implies the catalyst preserved ordered structure from the support. A well-defined step represents the spontaneous filling of the mesopores due to capillary condensation. For parent MCM-41 it occurred at $p/p_0 = 0.35$, and for M-*Pr*PPh_2Rh catalyst it occurred at $p/p_0 = 0.25$. This means the M-*Pr*PPh_2Rh catalyst requires lower pressure to establish multi-layer adsorption equilibrium, which is the result of the decreased pore size of the catalyst than support. The pore size distribution is very narrow, which shows the unique characters of template-synthesized mesoporous materials. Textual properties derived from the N_2 sorption analysis are summarized in Table 1.

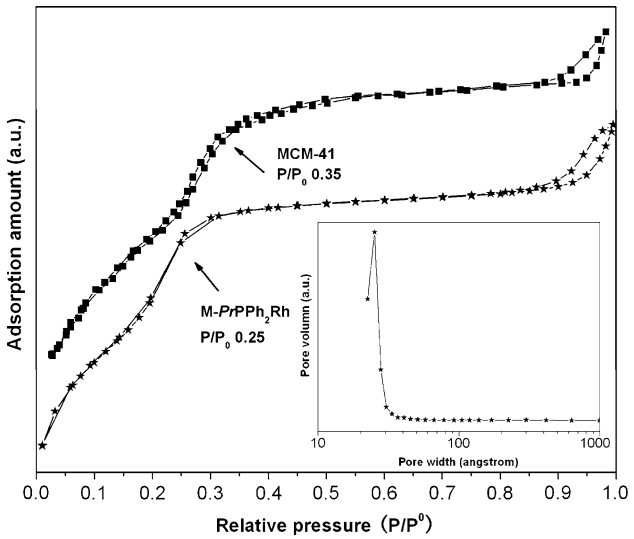

Fig. 3 Isotherms of parent MCM-41 (*square*) and M–*Pr*PPh_2Rh catalyst (*star*). Inset: pore size distribution plot of M–*Pr*PPh_2Rh catalyst

3.2 Hydroformylation of 1-Octene

1-Octene hydroformylation results over the M–*Pr*PPh_2Rh and S–*Pr*PPh_2Rh catalysts are shown in Table 2. Rhodium leaching from each catalyst cycle is also presented in table. M–*Pr*PPh_2Rh revealed high turnover number (TON) of 1-octene within several catalyst cycles. The selectivity of nonyl aldehydes was high (>97%). Total rhodium leaching for six recycles was 0.29%, which is lower than previous reports [6, 8]. Noticeably, the majority of leached rhodium was original from the first catalyst cycle, which might be those anchored on the external surface of MCM-41 [4]. The rhodium leaching is very low, as a consequence of more stable coordination of Rh–P complex than Rh–N complex. M–*Pr*PPh_2Rh also showed higher specific activity and obvious lower metal loss than the analogue catalyst S–*Pr*PPh_2Rh. This is probably attributable to the uniform pore size distribution of ordered mesoporous silicates that

Table 2 1-Octene hydroformylation over the catalysts[a]

Catalyst	Cycle	1-Octene Conv. (%)	1-Octene TON[b]	Seletivity of C_9 aldehydes (%)	*n*/*i*[c]	Rh loss[d] (%)
M–*Pr*PPh_2Rh (1.5 wt% Rh)	1	85.2	1,025	99.2	1.5	0.15
	2	84.5	1,017	98.8	1.4	0.05
	3	84.4	1,015	98.5	1.6	0.04
	4	84.7	1,019	99.0	1.5	0.02
	5	84.4	1,015	98.6	1.7	0.02
	6	83.0	998	97.5	1.8	0.01
S–*Pr*PPh_2Rh (0.8 wt% Rh)	1	45.0	902	99.9	1.3	0.40
	2	45.8	918	99.9	1.2	0.42
	3	45.6	915	99.7	1.3	0.33
	4	44.0	882	99.4	1.0	0.28

[a] Reaction temperature 393 K, reaction time 2.5 h, syngas ($CO/H_2 = 1$) 5 MPa. Toluene 15 mL, catalyst 0.18 g, 1-octene 5 mL

[b] TON (turnover number) = molar ratio of converted 1-octene and immobilized Rh

[c] Molar ratio of normal and branched nonyl aldehyde

[d] Weight ratio of rhodium leaching in reaction liquid with total immobilized rhodium on the catalyst used

nano SiO_2 particles, since the portion of linear nonyl aldehyde was also higher in M–*Pr*PPh_2Rh-catalyzed cases. The function of ordered mesopores upon sieving molecules is clear. M–*Pr*PPh_2Rh after six runs in 1-octene hydroformylation was characterized by XRD, and a well-resolved reflection was observed at $2\theta = 2.22°$ (Fig. 1c), indicating the catalyst structure was not ruined during the reaction.

Since propyl is electron-donating, the coordination of diphenylphosphinopropyl with rhodium (–*Pr*PPh_2–Rh) is stronger than that of triphenyl phosphine with rhodium (Ph_3P–Rh), which ensures the immobilization of rhodium during the hydroformylation of 1-octene. On the basis of the literature which described a detailed hydroformylation mechanism over homogenous rhodium complex [20], we infer that the 1-octene hydroformylation over the M–*Pr*PPh_2Rh catalyst has most likely occurred according to the dissociative mechanism as shown in Scheme 2. The reaction started with the addition of H_2 to M–*Pr*PPh_2Rh catalyst (a). After the orderly transformation of states (c), (d), and (e), 1-octene was coordinated by donating π electrons to the Rh empty orbit (f). The coordinated H could attack either of the C from the double bond. Then, through a series transformation of (g), (h), (i), and (j), linear nonyl aldehyde was received and the catalyst was regenerated to (c). Through (k), (l), (m), and (n), isomerized branched nonyl aldehyde was received the catalyst was also regenerated to (c). The hydroformylation results show a ratio of *n/i* nonyl aldehydes more than 1.5 (see Table 2). This is because isomerized nonyl aldehyde is larger than linear product and special hindrance took some effect inside the pores. As is discussed above, regarding the Rh–P coordination, –*Pr*PPh_2–Rh is stronger than Ph_3P–Rh. Consequently the dissociative phenyl phosphine will be triphenyl phosphine that is original from the complex precursor. In this case, immobilized rhodium is unlikely to be lost from the catalyst. As is shown in Scheme 2, since no triphenyl phosphine ligand was externally added, this ligand will be recycled during the reaction, (d) to (e) for dissociation, and (g) to (h) or (k) to (l) for addiction.

4 Conclusions

$RhCl(CO)(PPh_3)_2$ complex (Ph=phenyl) was successfully anchored to diphenylphosphinopropyl-modified mesoporous silicate MCM-41. The prepared catalyst preserves

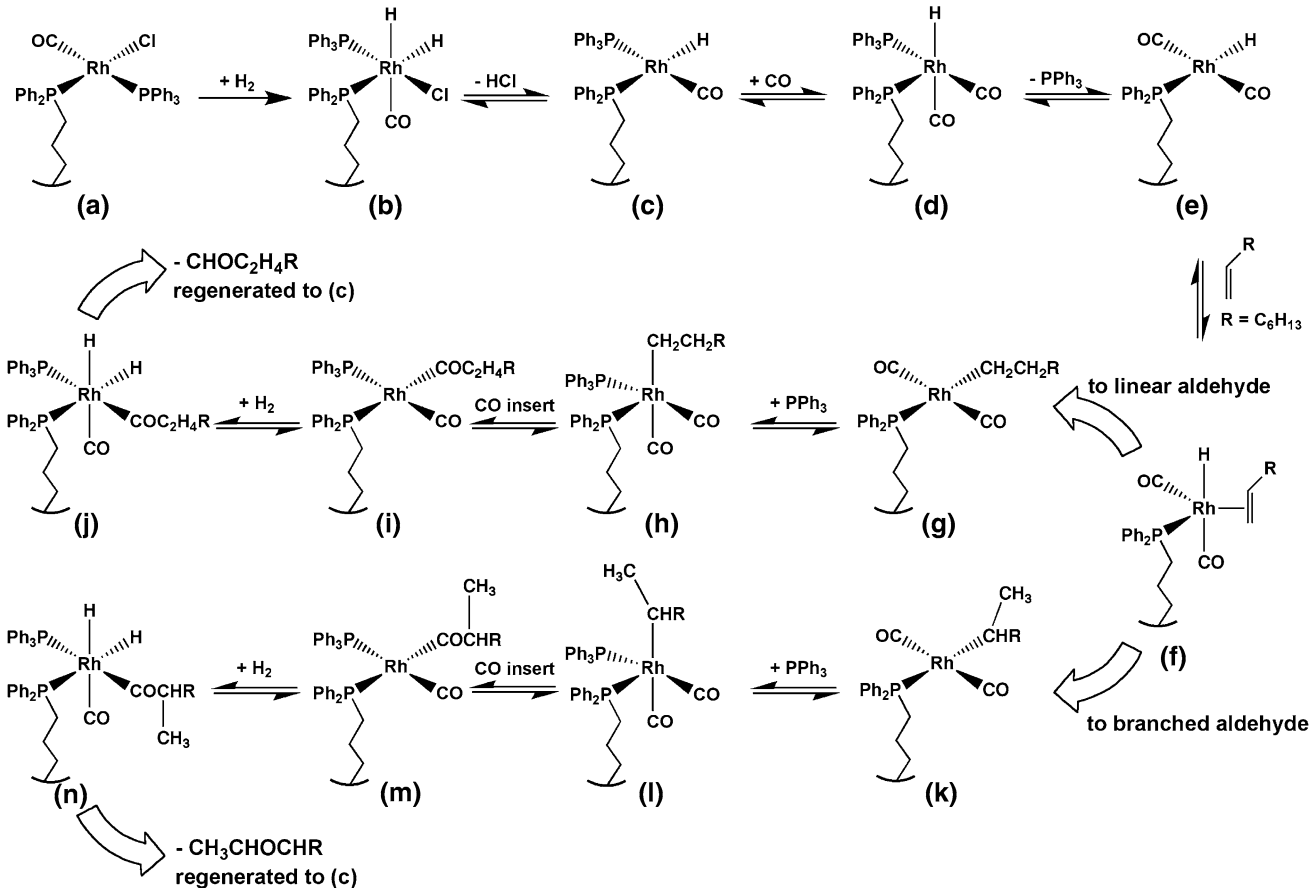

Scheme 2 A possible dissociative hydroformylation mechanism over the M–*Pr*PPh_2Rh catalyst

ordered hexagonal mesoporous structure of MCM-41. FT-IR spectroscopy was performed and critical absorptions were assigned to monitor the multi-assemble of Rh–P complex. The immobilized catalyst was employed in the hydroformylation of 1-octene. The catalyst showed high TON of substrate and high selectivity of nonyl aldehydes (>97%). Total Rh loss during six recycles of the catalyst was satisfyingly less than 0.3%. This might result from the stable Rh–P complex formed. The catalyst also shows higher activity and lower metal loss than analogue by nano SiO_2 as support, probably as a result of the confining of ordered mesoporous silicates upon molecule sieving.

Acknowledgments This work is financially supported by the National Natural Science Foundation of China (No. 20673064), Specialized Research Fund for the Doctoral Program of Higher Education of Ministry of Education of China (2007003108) and Fund for Analysis of Tsinghua University.

References

1. van Koten G, van Leeuwen PWNM (1999) In: van Santen RA, van Leeuwen PWNM, Moulijn JA, Averill RA (eds) Catalysis: an integrated approach, ch 6. Elsevier, Amsterdam
2. van Leeuwen PWNM, Claver C (eds) (2000) Rhodium catalyzed hydroformylation. Kluwer, Amsterdam
3. Corma A, Garcia H (2006) Adv Synth Catal 348:1391
4. Peng Q, Yang Y, Yuan Y (2004) J Mol Catal A: Chem 219:175
5. Huang L, He Y, Kawi S (2004) J Mol Catal A: Chem 213:241
6. Li P, Kawi S (2008) Catal Today 131:61
7. Marteel A, Davies JA, Mason MR, Tackb T, Bektesevic S, Abraham MA (2003) Catal Commun 4:309
8. Reek JNH, Kamer PCJ, Lutz M, Spek AL, van Leeuwen PWNM (1999) Angew Chem Int Ed 38:3231
9. Honaker MT, Sandefur BJ, Hargett JL, McDaniel AL, Salvatore RN (2003) Tetrahedron Lett 44:8373
10. Beck JS, Vartuli JC, Roth WJ, Leonowicz ME, Kresge CT, Schmitt KD, Chu CT-W, Olsen DH, Sheppard EW, McCullen SB, Higgins JB, Schlenker JL (1992) J Am Chem Soc 114:10834
11. Hao X-Y, Zhang Y-Q, Wang J-W, Zhou W, Zhang C, Liu S (2006) Microporous Mesoporous Mater 88:38
12. Zhang C, Zhou W, Liu S (2005) J Phys Chem B 109:24319
13. Zhou W, He D (2008) Chem Commun. doi:10.1039/B812910J
14. Dean J (ed) (1995) Analytical chemistry handbook. McGraw-Hill, Singapore (Sect. 6)
15. Tian B, Liu X, Yu C, Gao F, Luo W, Xie S, Tu B and Zhao D (2002) Chem Commun 1186
16. Bellamy LJ (ed) (1975) The infra-red spectra of complex molecules, ch 20. Chapman and Hall, London
17. Ning Y (ed) (2000) Characterization of organic compounds and organic spectroscopy, ch 7. The Science Press, Beijing
18. Zhao L, Wang S, Wu Y, Hou Q, Wang Y, Jiang S (2007) J Phys Chem C 111:18387
19. Sing KSW, Everett DH, Haul RAW, Moscou L, Pierotti RA, Rouque'rol J, Siemieniewska T (1985) Pure Appl Chem 57:603
20. Evans E, Osborn JA, Wilkinson G (1968) J Chem Soc A 3133